Conjugated Polymers

International Edition: DOI: 10.1002/anie.201602775
German Edition: DOI: 10.1002/ange.201602775

# Diketopyrrolopyrrole-based Conjugated Polymers Bearing Branched Oligo(Ethylene Glycol) Side Chains for Photovoltaic Devices

*Xingxing Chen, Zijian Zhang, Zicheng Ding, Jun Liu,* and Lixiang Wang**

***Abstract:*** *Conjugated polymers are essential for solution-processable organic opto-electronic devices. In contrast to the great efforts on developing new conjugated polymer backbones, research on developing side chains is rare. Herein, we report branched oligo(ethylene glycol) (OEG) as side chains of conjugated polymers. Compared with typical alkyl side chains, branched OEG side chains endowed the resulting conjugated polymers with a smaller π-π stacking distance, higher hole mobility, smaller optical band gap, higher dielectric constant, and larger surface energy. Moreover, the conjugated polymers with branched OEG side chains exhibited outstanding photovoltaic performance in polymer solar cells. A power conversion efficiency of 5.37% with near-infrared photoresponse was demonstrated and the device performance could be insensitive to the active layer thickness.*

Conjugated polymer semiconductors have received great attention because of their application in high-performance organic light-emitting diodes (OLEDs), organic field-effect transistors (OFETs), and polymer solar cells (PSCs).[1–4] Compared with inorganic semiconductors, the greatest advantage of conjugated polymer semiconductors is the solution processability, which is due to the attached flexible side chains. Side chains of conjugated polymers not only ensure solubility, but also affect the solid state morphology and consequently determine the device performance.[5] In contrast to the great efforts devoted to conjugated polymer backbones, research on developing new side chains is rare.[6,7] Recently, conjugated polymers with high charge carrier mobility in OFETs have been designed with novel side chains, such as alkyl chains with different branching sites,[6a] siloxane-terminated alkyl chains,[6b] urea-embedded alkyl chains,[6c] semifluoroalkyl chains,[6d] and hybrid alkyl/oligo-(ethylene glycol) chains.[6e]

A widely-used solubilizing moiety is the oligo(ethylene glycol) (OEG) chain, which is well-known for its hydrophilicity.[8] Conjugated polymers containing straight OEG side chains have already been developed and used in OLEDs, OFETs, and PSCs.[9] However, their device performance is always poor owing to the large hydrophilicity.[9] Hecht and Bunz et al. have reported conjugated polymers with branched OEG side chains, which are soluble in water with high fluorescence quantum efficiency and can be used for biosensing.[10] Recently, we have discovered that OEG side chains are more flexible than alkyl chains and that they can facilitate π-π stacking of conjugated polymer backbones.[11]

For typical conjugated polymers bearing alkyl chains, branched alkyl chains generally lead to better solubility and improved device performance than those of straight alkyl chains.[5] This motivates us to develop branched OEG as side chains of conjugated polymers for PSC device application. Owing to the larger flexibility of OEG chains than that of alkyl chains (Scheme 1 a), the resulting conjugated polymers exhibit smaller π-π distances, and consequently redshifted absorption spectra and higher charge carrier mobility than the counterparts with branched alkyl chains. As a result, the conjugated polymers with branched OEG side chains can be used as donor materials in PSCs. The PSC device shows near-

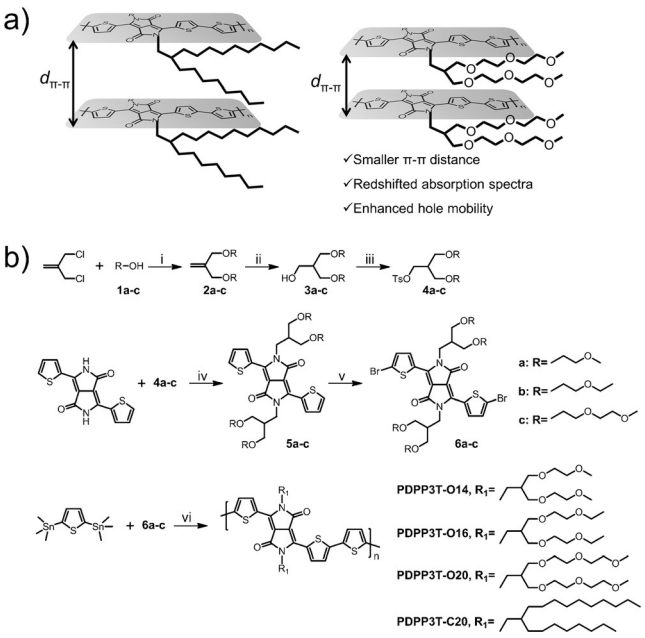


***Scheme 1.*** a) Illustration of the effect of branched OEG side chains. b) Chemical structures and synthetic routes of PDPP3T-O14, PDPP3T-O16, PDPP3T-O20, and PDPP3T-C20. (Reagents and conditions: i) NaH, THF, 0 °C and then 65 °C; ii) $BH_3$/THF, NaOH (aq), $H_2O_2$ (aq), r.t.; iii) $(CH_3)_3N{\cdot}HCl$, 4-toluene sulfonyl chloride, $Et_3N$, r.t.; iv) $K_2CO_3$, $(C_4H_9)_4NBr$, dimethylformamide, 120 °C; v) *N*-bromosuccinimide, dichloromethane, r.t.; vi) $Pd_2(dba)_3$, P(*o*-tolyl)$_3$, chlorobenzene/DMF (10:1, *v*/*v*), 135 °C.).

[*] X. Chen, Z. Zhang, Dr. Z. Ding, Prof. J. Liu, Prof. L. Wang
State Key Laboratory of Polymer Physics and Chemistry
Changchun Institute of Applied Chemistry
Chinese Academy of Sciences
Changchun 130022 (P.R. China)
E-mail: liujun@ciac.ac.cn
lixiang@ciac.ac.cn
X. Chen, Z. Zhang
University of Chinese Academy of Sciences
Beijing 100049 (P.R. China)

Supporting information for this article can be found under: http://dx.doi.org/10.1002/anie.201602775.

  

infrared (NIR) photoresponse with power conversion efficiency (PCE) of 5.37 %, which is among the highest reported for PSCs with NIR response. Moreover, these polymers enable PSCs with thick active layer, which are desirable for roll-to-roll manufacturing of PSCs. These results demonstrate the promising application of branched OEG as side chains of conjugated polymers.

The chemical structures and synthetic routes of the polymers are shown in Scheme 1 b. With poly((2,5-diyl-2,3,5,6-tetrahydro-3,6-dioxo-pyrrolo(3,4-c)pyrrole-1,4-diyl)-*alt*-(2,2′:5′,2″-terthiophene-5,5″-diyl)) (PDPP3T)[12] as the conjugated polymer backbone, we incorporate branched OEG of different length as the side chains to develop the polymers, PDPP3T-O14, PDPP3T-O16 and PDPP3T-O20. For comparison, we synthesized the control polymer with alkyl side chains, PDPP3T-C20. As shown in Scheme 1 b, alcohol of the branched OEG chains were prepared by the substitution reaction with commercially available 3-chloro-2-(chloromethyl)prop-1-ene and hydroboration-oxidation reaction with $BH_3/H_2O_2$. Tosylation and subsequent alkylation with 3,6-bis(thiophen-2-yl)-2*H*,5*H*-pyrrolo[3,4-*c*]pyrrole-1,4-dione afforded the compound **5a–c**, which was finally brominated to give the key monomer **6a–c**. The polymers were synthesized using Stille polycondensation of the key monomer **6a–c** and 2,5-bis(trimethylstannyl)thiophene.

PDPP3T-O14, PDPP3T-O16, and PDPP3T-O20 all exhibit good solubility in typical chlorinated solvents, such as chloroform and *o*-dichlorobenzene (*o*-DCB). Their chemical structures were confirmed by $^1$H NMR and elemental analysis. As listed in Table 1, PDPP3T-O14 and PDPP3T-O16 have high number-average molecular weight ($M_n$) of approximately 90000 g mol$^{-1}$ while PDPP3T-O20 has relatively low $M_n$ of 30000 g mol$^{-1}$. This is probably due to the difficulty to get high purity monomer **6c**, which is sticky liquid and cannot be purified by recrystallization. All of the polymers exhibit good thermal stability with thermal degradation temperature ($T_d$) higher than 360 °C.

Branched OEG side chains facilitate close π-π stacking of the conjugated polymer backbone. According to the grazing incidence X-ray diffraction (GI-XRD) pattern (Figure 1 a), the π-π stacking distance of polymer backbone ($d_{\pi\text{-}\pi}$) is 3.80 Å for PDPP3T-C20 and 3.60 Å for PDPP3T-O14, PDPP3T-O16, and PDPP3T-O20. The decreased $d_{\pi\text{-}\pi}$ with OEG side chains is due to the more flexibility of OEG chain compared to alkyl chain.[9] As the stacking distance of the alkyl chain (4.1 Å) is larger than that of ideal π-π stacking distance (ca. 3.4 Å),[13] alkyl side chains act as steric hindrance and prevent the close π-π stacking of conjugated polymer backbones in the solid state. The flexible branched OEG side chains alleviate the steric hindrance effect, thus favoring the π-π stacking of conjugated polymer backbone.

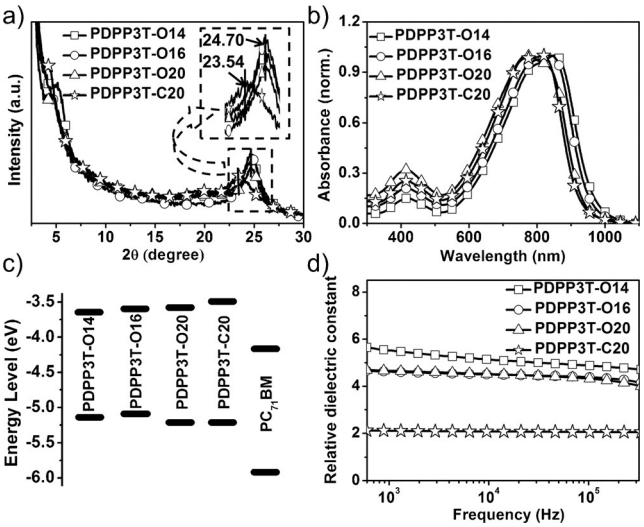


***Figure 1.*** a) GI-XRD patterns of the spin-coated films of the four polymers. b) UV/Vis absorption spectra of the four polymers in thin film. c) LUMO/HOMO energy levels of the four polymers estimated from CV measurement. d) Dependence of $\varepsilon_r$ on frequency of the four polymers.

***Table 1:*** Molecular weight, photophysical properties, electrochemical properties, LUMO/HOMO energy levels, π-π stacking distance, dielectric constants, hole mobilities, and surface energies of the four polymers.

| | PDPP3T-O14 | PDPP3T-O16 | PDPP3T-O20 | PDPP3T-C20 |
|---|---|---|---|---|
| $M_n$ (kg mol$^{-1}$) | 96 | 92 | 30 | 95 |
| $M_w$ (kg mol$^{-1}$) | 214 | 205 | 154 | 228 |
| PDI | 2.23 | 2.20 | 5.16 | 2.40 |
| $\lambda_{max}^{sol}$ (nm) | 807 | 807 | 734 | 807 |
| $\lambda_{max}^{film}$ (nm) | 853 | 841 | 825 | 819 |
| $E_g^{opt}$ (eV) | 1.28 | 1.30 | 1.33 | 1.34 |
| $E_{onset,}^{red}$ (eV) | −1.15 | −1.19 | −1.20 | −1.30 |
| $E_{onset,}^{ox}$ (eV) | 0.33 | 0.29 | 0.41 | 0.40 |
| $E_{LUMO}$ (eV) | −3.65 | −3.61 | −3.60 | −3.50 |
| $E_{HOMO}$ (eV) | −5.13 | −5.09 | −5.21 | −5.20 |
| $\varepsilon_r$ | 5.5 ± 0.3 | 4.6 ± 0.2 | 4.6 ± 0.2 | 2.0 ± 0.1 |
| $d_{\pi\text{-}\pi}$ (Å) | 3.60 | 3.60 | 3.60 | 3.80 |
| $\mu_h$ (cm$^2$ V$^{-1}$ s$^{-1}$) | $4.14\times10^{-3}$ | $2.53\times10^{-3}$ | $1.10\times10^{-3}$ | $1.55\times10^{-3}$ |
| $\gamma$ (mJ m$^{-2}$) | 44.03 | 35.27 | 60.59 | 24.72 |

As shown in Figure 1 b, the absorption spectra of thin films of PDPP3T-O14 and PDPP3T-O16 are redshifted compared to that of PDPP3T-C20. Because these polymers have the same polymer backbone, the redshifted absorption spectra are attributed to the strong interaction of conjugated polymer backbones in the solid state. The decreased π-π stacking distance with branched OEG side chains should contribute to the strong interaction of polymer backbones. PDPP3T-O14 and PDPP3T-O16 show strong absorption in the NIR region with the absorption maxima at 853 nm and 841 nm, respectively. The HOMO/LUMO energy levels of the four polymers were estimated with the onset oxidation/reduction potentials in cyclic voltammetry. As shown in Figure 1 c, the polymers with branched OEG side chains generally exhibited higher-lying HOMO levels and lower-lying LUMO levels than those of PDPP3T-C20 with alkyl side chains.

To investigate the effect of OEG side chains on charge carrier mobility, we measured the hole mobility ($\mu_h$) of the four polymers using the space-charge-limited current (SCLC) method with the hole-only devices (device structure: ITO/PEDOT:PSS/polymer/$MoO_3$/Ag). As listed in Table 1, the hole mobility of PDPP3T-O14 ($\mu_h = 4.14\times10^{-3}$ cm$^2$ V$^{-1}$ s$^{-1}$) and PDPP3T-O16 ($\mu_h = 2.53\times10^{-3}$ cm$^2$ V$^{-1}$ s$^{-1}$) are higher

  

than that of PDPP3T-C20 ($\mu_h = 1.55 \times 10^{-3}\ cm^2 V^{-1} s^{-1}$). This was attributed to the smaller $d_{\pi\text{-}\pi}$ with OEG side chains, which facilitate the intermolecular charge carrier hopping. This result confirmed that hydrophilic OEG side chains do not decrease the charge transporting properties of hydrophobic conjugated polymer backbones. Comparison of the hole mobility of the three polymers containing branched OEG side chains indicated that increased OEG side chain length led to decreased hole mobility.

Branched OEG side chains lead to an increased $\varepsilon_r$ of the resulting polymers. PCE of PSCs lags behind that of inorganic solar cells owing to the low $\varepsilon_r$ of organic/polymer semiconductors.[14] In comparison to inorganic semiconductors with a large $\varepsilon_r$ and small exciton binding energy, organic/polymer semiconductors typically have a low $\varepsilon_r$ (in the range of 2–4) and a large exciton binding energy. The large exciton binding energy leads to significant recombination loss and limits PCE of PSCs. The $\varepsilon_r$ of the polymers was estimated using impedance spectroscopy with the capacitance devices (device structure: ITO/PEDOT:PSS/polymer/Al). As shown in Figure 1 d, the $\varepsilon_r$ in the range of 100 Hz to 1 MHz of PDPP3T-O14, PDPP3T-O16, and PDPP3T-O20 with branched OEG side chains is $5.5 \pm 0.3$, $4.6 \pm 0.2$, and $4.6 \pm 0.2$, respectively, which are much higher than that of PDPP3T-C20 with alkyl side chains ($\varepsilon_r = 2.0 \pm 0.1$; Table 1).[15] The enhanced $\varepsilon_r$ is due to the large dipole moment of the C–O unit and the flexibility of the OEG chains, which make the dipole moment readily response to the applied electrical field.[15] The high $\varepsilon_r$ of the polymers containing branched OEG side chains indicated their great potential for high-efficiency PSCs.

Branched OEG side chains increase the surface energy ($\gamma$) of the resulting polymers. As listed in Table 1, the surface energies of PDPP3T-O14, PDPP3T-O16, and PDPP3T-O20 with branched OEG side chains are 44.0, 35.3, and 60.6 $mJ\,m^{-2}$, respectively, which are higher than that of PDPP3T-C20 with alkyl side chains ($\gamma = 24.7\ mJ\,m^{-2}$; Table 1). This was attributed to the larger polarity of OEG chains than that of alkyl chains. Surface energy affects the compatibility of two materials and plays an important role in the phase separation of the blend.[16] A typical acceptor material, [6,6]-phenyl-$C_{71}$-butyric acid methyl ester ($PC_{71}BM$), has the surface energy of 34.2 $mJ\,m^{-2}$.[16b] Despite the increased surface energies with OEG side chains, the surface energies of PDPP3T-O14 and PDPP3T-O16 are close to that of $PC_{71}BM$, suggesting that the two polymers should have compatibility with $PC_{71}BM$ to give good blend morphology.

To evaluate the photovoltaic properties of the four polymers, PSC devices were fabricated with the configuration of ITO/PEDOT:PSS/polymer:$PC_{71}BM$/Ca/Al. For PDPP3T-O16, PDPP3T-O20, and PDPP3T-C20, the active layer was spin-coated from the solution in *o*-DCB containing 3 vol% 1,8-diiodooctane (DIO). As PDPP3T-O14 gelated in *o*-DCB at room temperature, the active layer of PDPP3T-O14:$PC_{71}BM$ was obtained from the *o*-DCB solution at 120 °C.

The current density–voltage (*J*-*V*) curves of the devices under illumination with a light intensity of 100 $mW\,cm^{-2}$ with an AM 1.5G filter are shown in Figure 2 a and the photovoltaic parameters are listed in Table 2. Among the four polymers, PDPP3T-O16 exhibits the best device performance with the open-circuit voltage ($V_{OC}$) of 0.57 V, short-circuit current density ($J_{SC}$) of 14.30 $mA\,cm^{-2}$, fill factor (FF) of 66%, corresponding to power conversion efficiency (PCE) of 5.37%. This PCE is very comparable to those reported for polymer donors with the same conjugated backbone and alkyl side chains, indicating that branched OEG side chains of donor polymers do not decrease PSC device performance. PDPP3T-O14 and PDPP3T-O16 exhibit better photovoltaic performances than that of PDPP3T-O20 and PDPP3T-C20 owing to the improved active layer morphology. As shown in the transmission electron microscopy (TEM) images (Figure 3), large size aggregation can be observed in the active layers of PDPP3T-O20 and PDPP3T-C20, leading to poor exciton diffusion/dissociation. In comparison, fine and interconnecting fibrillar structures were achieved for the active layers of PDPP3T-O14 and PDPP3T-O16. The good blend morphology of PDPP3T-O14 and PDPP3T-O16 is attributed to good compatibility of the two polymers with $PC_{71}BM$, which is consistent with their similar surface energy.

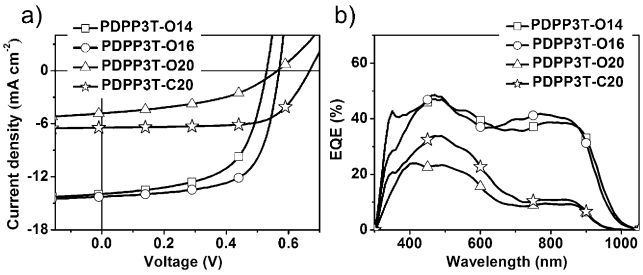


***Figure 2.*** a) *J*-*V* and b) EQE curves of the PSC devices based on the four polymers with the active layer thickness of ca. 100 nm.

***Table 2:*** Characteristics of the PSC devices of the four polymers.

| Donor | Thickness [nm] | $V_{OC}$ [V] | $J_{SC}$ [$mA\,cm^{-2}$] | FF [%] | PCE [%] |
|---|---|---|---|---|---|
| PDPP3T-O14 | 103 | 0.53 | 13.95 | 59.8 | 4.42 |
| PDPP3T-O16 | 100 | 0.57 | 14.30 | 66.0 | 5.37 |
| PDPP3T-O20 | 70 | 0.56 | 4.82 | 44.3 | 1.20 |
| PDPP3T-C20 | 84 | 0.68 | 6.45 | 68.1 | 3.00 |
| PDPP3T-O14 | 210 | 0.50 | 16.42 | 55.0 | 4.52 |
| PDPP3T-O14 | 290 | 0.50 | 17.48 | 49.0 | 4.29 |

PSCs with near infrared (NIR) photoresponses can efficiently harvest solar photons and are very desirable for tandem solar cells.[17] It is challenging to develop ultra-small band gap polymers for efficient, NIR photoresponive PSCs because of the difficulty in managing LUMO/HOMO levels of the polymers.[17] According to the external quantum efficiency (EQE) spectra shown in Figure 2 b, the devices of PDPP3T-O14 and PDPP3T-O16 exhibit strong responses in the NIR region up to 1000 nm. In a wide range of 400–900 nm, the overall EQE is about 0.4. Notably, the PCE of 5.37% for PDPP3T-O16 is among the highest reported for PSCs with a NIR photoresponse.[17]

A thick active layer (> 200 nm) of PSCs is necessary for roll-to-roll manufacturing of PSCs.[18] Usually, increasing the

  

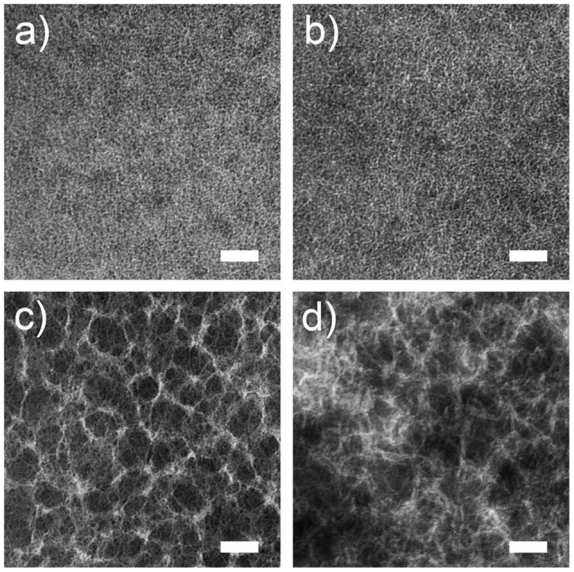


***Figure 3.*** TEM images of the active layers with the thickness of about 100 nm based on the blends of the four polymers with $PC_{71}BM$. The scale bar is 200 nm.

thickness beyond 100 nm leads to increased bimolecular charge recombination and consequently decreased FF. Only a limited number of polymer donors can enable PSC devices with thick active layer while maintaining high FF and PCE.[18] We tested the PSC devices of PDPP3T-O14 with different active layer thicknesses by adjusting the spin-coating speed. As shown in Figure 4 and listed in Table 2, with the thickness increasing from 103 nm to 290 nm, the $J_{SC}$ increases slightly and the FF decreases slightly, thus maintaining the PCE in the range of 4.2–4.5%. The insensitivity of the active layer thickness is attributed to the high hole mobility of PDPP3T-O14 and the interconnecting fibrillar morphology of the active layer.[18b,c]

In summary, we have developed a series of conjugated polymers bearing branched OEG side chains. Compared with the corresponding polymer with alkyl side chains, the conjugated polymer with branched OEG side chains exhibit a smaller π-π stacking distance, higher hole mobility, red-shifted absorption spectrum, higher dielectric constant, and larger surface energy. The resulting PSC devices exhibited photoresponses in the infrared region with PCE of 5.37%. Moreover, PCE of the device of PDPP3T-O14 was insensitive to the active layer thickness. The enhanced dielectric constant, good PSC device efficiency, and insensitivity to active layer thickness suggest that branched OEG side chains are a promising substitute for widely used alkyl side chains.

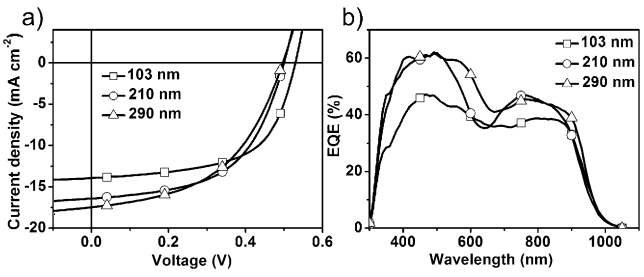


***Figure 4.*** a) *J-V* and b) EQE curves of the PSC devices based on PDPP3T-O14:$PC_{71}BM$ active layer with different thickness.

## *Acknowledgements*

The authors are grateful for the financial support by the 973 Project (No. 2014CB643504, 2015CB655001), the Nature Science Foundation of China (No. 51373165), the "Thousand Talents Program" of China, and the Strategic Priority Research Program of the Chinese Academy of Sciences (No. XDB12010200).

**Keywords:** conjugated polymers · dielectric constants · oligo(ethylene glycol) · side chains · solar cells

**How to cite:** *Angew. Chem. Int. Ed.* **2016**, *55*, 10376–10380
*Angew. Chem.* **2016**, *128*, 10532–10536

[1] A. J. Heeger, *Chem. Soc. Rev.* **2010**, *39*, 2354–2371.
[2] J. Liu, Q. Zhou, Y. Cheng, Y. Geng, L. Wang, D. Ma, X. Jing, F. Wang, *Adv. Mater.* **2005**, *17*, 2974–2978.
[3] S. Holliday, J. E. Donaghey, I. McCulloch, *Chem. Mater.* **2014**, *26*, 647–663.
[4] a) Y. Li, *Acc. Chem. Res.* **2012**, *45*, 723–733; b) L. Lu, T. Zheng, Q. Wu, A. M. Schneider, D. Zhao, L. Yu, *Chem. Rev.* **2015**, *115*, 12666–12731.
[5] a) T. Lei, J.-Y. Wang, J. Pei, *Chem. Mater.* **2014**, *26*, 594–603; b) J. Mei, Z. Bao, *Chem. Mater.* **2014**, *26*, 604–615; c) H. Zhou, L. Yang, W. You, *Macromolecules* **2012**, *45*, 607–632; d) P. M. Beaujuge, J. M. J. Fréchet, *J. Am. Chem. Soc.* **2011**, *133*, 20009–20029.
[6] a) T. Lei, J.-H. Dou, J. Pei, *Adv. Mater.* **2012**, *24*, 6457–6461; b) J. Mei, D. H. Kim, A. L. Ayzner, M. F. Toney, Z. Bao, *J. Am. Chem. Soc.* **2011**, *133*, 20130–20133; c) J. Yao, C. Yu, Z. Liu, H. Luo, Y. Yang, G. Zhang, D. Zhang, *J. Am. Chem. Soc.* **2016**, *138*, 173–185; d) R. Kim, B. Kang, D. H. Sin, H. H. Choi, S.-K. Kwon, Y.-H. Kim, A. K. Cho, *Chem. Commun.* **2015**, *51*, 1524–1527; e) B. Kang, R. Kim, S. B. Lee, S.-K. Kwon, Y.-H. Kim, K. Cho, *J. Am. Chem. Soc.* **2016**, *138*, 3679–3686.
[7] a) F. Huang, H. Wu, D. Wang, W. Yang, Y. Cao, *Chem. Mater.* **2004**, *16*, 708–716; b) G. Zhou, G. Qian, L. Ma, Y. Cheng, Z. Xie, L. Wang, X. Jing, F. Wang, *Macromolecules* **2005**, *38*, 5416–5424; c) H. Zhou, Y. Zhang, C.-K. Mai, S. D. Collins, T.-Q. Nguyen, G. C. Bazan, A. J. Heeger, *Adv. Mater.* **2014**, *26*, 780–785.
[8] a) W.-S. Li, Y. Yamamoto, T. Fukushima, A. Saeki, S. Seki, S. Tagawa, H. Masunaga, S. Sasaki, M. Takata, T. Aida, *J. Am. Chem. Soc.* **2008**, *130*, 8886–8887; b) X. Zhang, Z. Chen, F. Würthner, *J. Am. Chem. Soc.* **2007**, *129*, 4886–4887.
[9] a) M. Shao, Y. He, K. Hong, C. M. Rouleau, D. B. Geohegan, K. Xiao, *Polym. Chem.* **2013**, *4*, 5270–5274; b) M. Breselge, I. V. Severen, L. Lutsen, P. Adriaensens, J. Manca, D. Vanderzande, T. Cleij, *Thin Solid Films* **2006**, *511*, 328–332.
[10] a) A. Khan, S. Muller, S. Hecht, *Chem. Commun.* **2005**, 584–586; b) R. L. Phillips, I.-B. Kim, L. M. Tolbert, U. H. F. Bunz, *J. Am. Chem. Soc.* **2008**, *130*, 6952–6955; c) R. L. Phillips, O. R. Miranda, C.-C. You, V. M. Rotello, U. H. F. Bunz, *Angew. Chem. Int. Ed.* **2008**, *47*, 2590–2594; *Angew. Chem.* **2008**, *120*, 2628–2632.
[11] B. Meng, H. Song, X. Chen, Z. Xie, J. Liu, L. Wang, *Macromolecules* **2015**, *48*, 4357–4363.

  

[12] J. C. Bijleveld, A. P. Zoombelt, S. G. J. Mathijssen, M. M. Wienk, M. Turbiez, D. M. de Leeuw, R. A. J. Janssen, *J. Am. Chem. Soc.* **2009**, *131*, 16616 – 16617.
[13] R. Boese, H. C. Weiss, D. Bläser, *Angew. Chem. Int. Ed.* **1999**, *38*, 988 – 992; *Angew. Chem.* **1999**, *111*, 1042 – 1045.
[14] a) L. J. A. Koster, S. E. Shaheen, J. C. Hummelen, *Adv. Energy Mater.* **2012**, *2*, 1246 – 1253; b) S. Chen, S.-W. Tsang, T.-H. Lai, J. R. Reynolds, F. So, *Adv. Mater.* **2014**, *26*, 6125 – 6131.
[15] S. Torabi, F. Jahani, I. V. Severen, C. Kanimozhi, S. Patil, R. W. A. Havenith, R. C. Chiechi, L. Lutsen, D. J. M. Vanderzande, T. J. Cleij, J. C. Hummelen, L. J. A. Koster, *Adv. Funct. Mater.* **2015**, *25*, 150 – 157.
[16] a) X. Bulliard, S.-G. Ihn, S. Yun, Y. Kim, D. Choi, J.-Y. Choi, M. Kim, M. Sim, J.-H. Park, W. Choi, K. Cho, *Adv. Funct. Mater.* **2010**, *20*, 4381 – 4387; b) J. Lee, M. Kim, B. Kang, S. B. Jo, H. G. Kim, J. Shin, K. Cho, *Adv. Energy Mater.* **2014**, *4*, 1400087; c) B. H. Lee, J. Shim, G. Kim, H. Kim, S. Song, H. Suh, K. Lee, *Appl. Phys. Lett.* **2012**, *101*, 083304; d) Y. Sun, S.-C. Chien, H.-L. Yip, K.-S. Chen, Y. Zhang, J. A. Davies, F.-C. Chen, B. Lin, A. K.-Y. Jen, *J. Mater. Chem.* **2012**, *22*, 5587 – 5595.
[17] a) K. H. Hendriks, W. Li, M. M. Wienk, R. A. J. Janssen, *J. Am. Chem. Soc.* **2014**, *136*, 12130 – 12136; b) T. T. Steckler, P. Henriksson, S. Mollinger, A. Lundin, A. Salleo, M. R. Andersson, *J. Am. Chem. Soc.* **2014**, *136*, 1190 – 1193; c) T. L. D. Tam, T. Salim, H. Li, F. Zhou, S. G. Mhaisalkar, H. Su, Y. M. Lam, A. C. Grimsdale, *J. Mater. Chem.* **2012**, *22*, 18528 – 18534.
[18] a) W. Li, K. H. Hendriks, W. S. C. Roelofs, Y. Kim, M. M. Wienk, R. A. J. Janssen, *Adv. Mater.* **2013**, *25*, 3182 – 3186; b) J. Gao, L. Dou, W. Chen, C.-C. Chen, X. Guo, J. You, B. Bob, W.-H. Chang, J. Strzalka, C. Wang, G. Li, Y. Yang, *Adv. Energy Mater.* **2014**, *4*, 1300739; c) Z. Chen, P. Cai, J. Chen, X. Liu, L. Zhang, L. Lan, J. Peng, Y. Ma, Y. Cao, *Adv. Mater.* **2014**, *26*, 2586 – 2591.

Received: March 19, 2016
Revised: May 3, 2016
Published online: June 3, 2016

  